Supporting Information

Pyreneacyl Sulfides as a Visible Light-Induced Versatile Ligation Platform

Bryan T. Tuten,[a] Jan P. Menzel,[a] Kai Pahnke,[a] James Blinco,[b]* and Christopher Barner-Kowollik[a,b]*

[a]Preparative Macromolecular Chemistry, Institut für Technische Chemie und Polymerchemie, Karlsruhe Institute of Technology (KIT), Engesserstr. 18, 76131 Karlsruhe, Germany

[b]School of Chemistry, Physics and Mechanical Engineering, Queensland University of Technology (QUT), 2 George Street, Brisbane, QLD 4001, Australia

Table of Contents

1.) General

Materials

Dichloromethane (DCM, 99.8% extra dry, Arcos), tetrahydrofuran (THF, 99.8%, extra dry, Acros), 1-bromoacetylpyrene (97%, Sigma-Aldrich), thioglycolic acid (98% Sigma-Aldrich), dicylcopenadiene (90%, stabilized, ABCR), butylamine (99.5%, Sigma-Aldrich), 4-chlorobenzyl mercaptan (98%, Sigma-Aldrich), O-(2,3,4,5,6-pentafluorobenzyl)hydroxylamine hydrochloride (99+%, Alfa Aesar), 4-(dimethylamino)pyridine (DMAP, 99+%, Sigma-Aldrich), N,N'-dicyclohexylcarbodiimide (DCC, 99%, Alfa Aesar), *tert*-butyl methacrylate (Sigma-Aldrich, 98 %) and *tert*-butyl acrylate (Sigma-Aldrich, 99 %) were deinhibited via a short column of basic aluminum oxide. Copper(I) iodide (Sigma-Aldrich, ≥ 98 %), tin(II) 2-ethylhexanoate (Sigma-Aldrich, 95 %), tris[2-(dimethylamino)ethyl]amine (Sigma-Aldrich, 97 %), butylene bis(2-bromoisobutyrate) (provided by Evonik Industries), ethyl α-bromoisobutyrate (Sigma Aldrich, 98 %), triphenylphosphine and sodium iodide (ABCR, 99 %) were used as received. Nickelocene (ABCR, 99 %) was used as received and handled in a glovebox.

Characterization

^{1}H NMR, ^{13}C NMR, and ^{19}F NMR spectroscopy was performed using a Bruker Ascend 400 at 400 MHz. All samples were dissolved in deuterated dimethylsulfoxide (DMSO-d^6 or deuterated chloroform ($CDCl_3$). The δ-scale is referenced to the internal standard tetramethylsilane (TMS, δ = 0.00 ppm).

ESI-MS (Electrospray Ionization Mass Spectrometry) spectra were recorded on a Q Exactive (Orbitrap) mass spectrometer (ThermoFisher Scientific, San Jose, CA, USA) equipped with an HESI II probe. The instrument was calibrated in the m/z range of 74-1822 using a premixed standard comprising caffeine, Met-Arg-Phe-Ala acetate (MRFA), and a mixture of fluorinated phosphazenes (Ultramark 1621). A constant spray voltage of 4.6 kV and a dimensionless sweep gas flow rate of 5 were applied. The capillary temperature and the S-lens RF level were set to 320 °C and 62.0, respectively. The samples were dissolved with a concentration of 0.05 mg·mL^{-1} in a mixture of THF and MeOH (3:2) containing 100 μmol sodium trifluoracetate (NaTFA). The samples were infused with a flow rate of 5 μL·min^{-1}.

Gel Permeation Chromatography (GPC) measurements were performed on a Polymer Laboratories (Varian) PL-GPC 50 Plus Integrated System, comprising an autosampler, a PLgel 5 mm bead-size guard column (50 x 7.5 mm), one PLgel 5mm Mixed E column (300 x 7.5 mm), three PLgel 5mm Mixed C columns (300 x 7.5 mm) and a differential refractive index detector using THF as the eluent at 35 °C with a flow rate of 1 mL min^{-1}. The present GPC system was calibrated using linear poly(methyl methacrylate) standards ranging from 700 to 2·106 g mol^{-1}. The resulting molar mass distributions were determined by universal calibration using Mark-Houwink parameters for poly(methyl methacrylate) (K = 12.8·10-5 dL g^{-1}, α = 0.69).[1]

UV/vis spectra were recorded in tetrahydrofuran/methanol (3:2 v/v) on a Varian Cary 300 Bio spectrophotometer.

Irradiation

Irradiations for visible light experiments were carried out with three light emitting diodes (Avonec, 410-420 nm, 3 W, actinic blue) at a distance of 2.5 cm from the sample vial, see Figure S1. During irradiation and stirring, the entire setup was covered by a protective box. Laser irradiation experiments were carried out with an Innolas Tunable Laser System SpitLight 600 OPO. An optical parametric oscillator (OPO) was pumped with a diode pumped Nd:YAG laser (repetition rate 100Hz). The energy output of the laser was down-regulated by a continuously variable attenuator (polarizer).

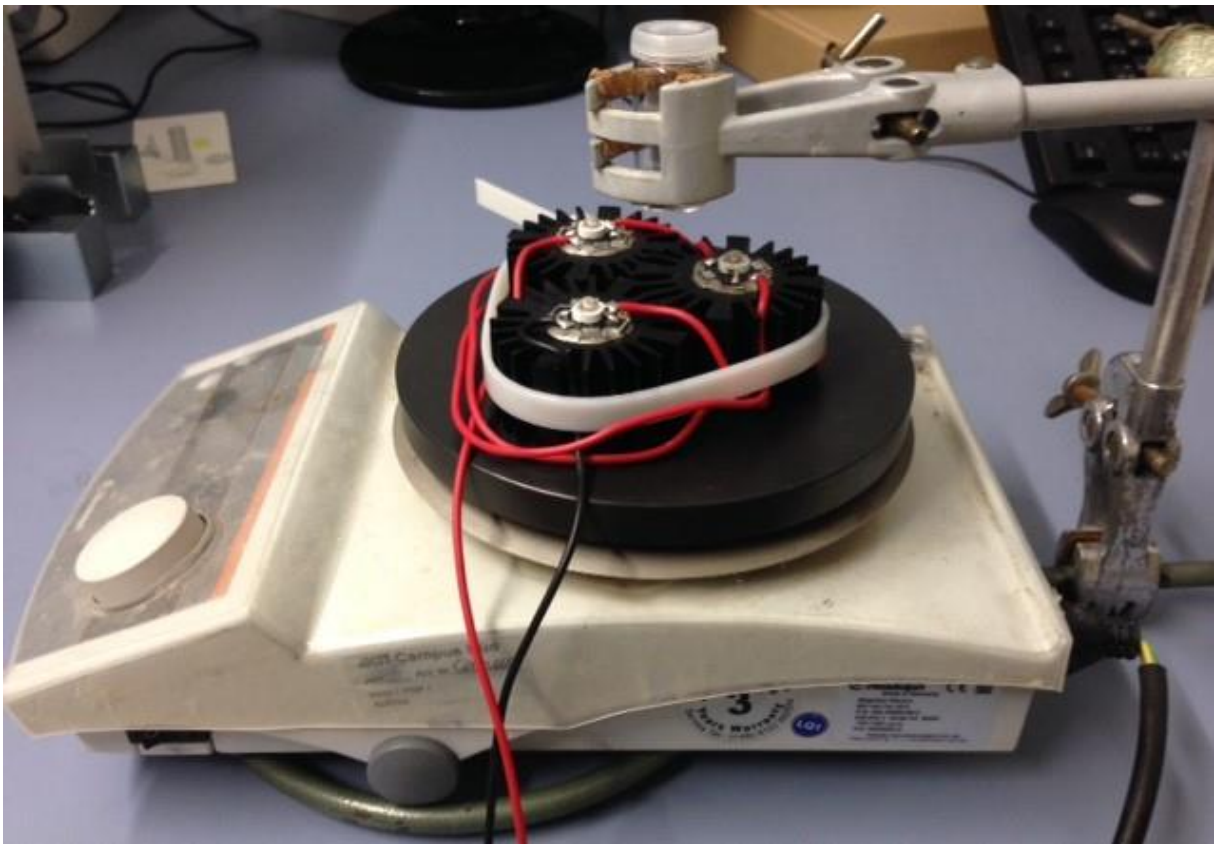

Figure S1: Visible light LED setup.

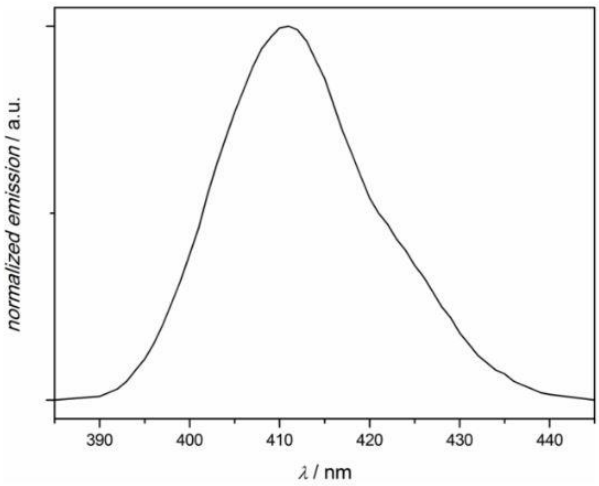

Figure S2: Emission spectrum of the employed blue light LEDs.

2.) Synthesis

Pyreneacyl sulfide terminated poly(ethylene glycol)

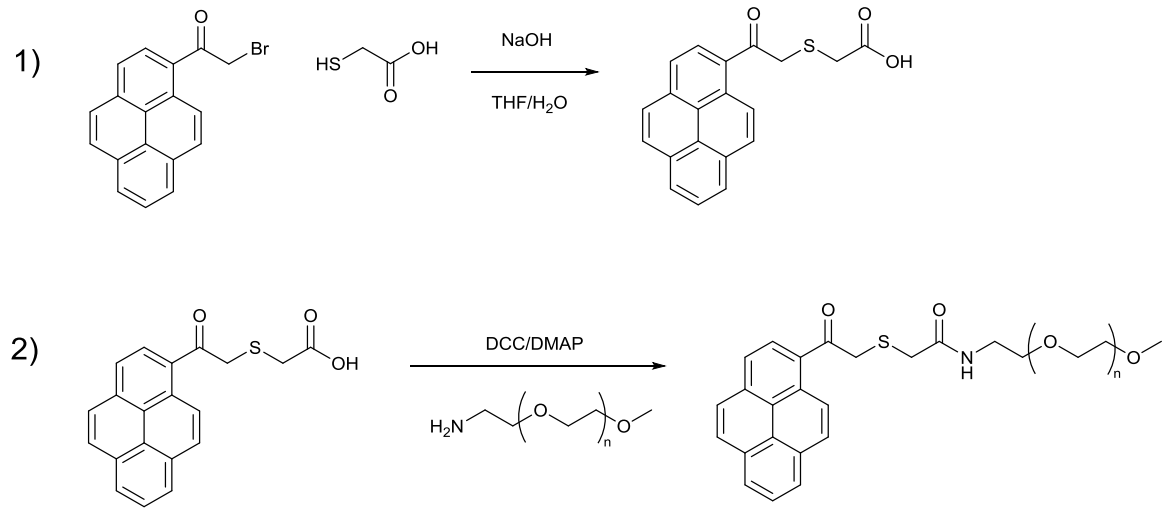

Scheme S1: Step 1, Synthesis of pyreneacyl sulfide acid precursor. Step 2, DCC coupling of the pyreneacyl sulfide acid precursor to monoamino-PEG

Step 1: A round bottom flask submerged in an ice bath was charged with 0.78 g (19.5 mmol) of NaOH and 30 mL of D.I. water. When all NaOH was dissolved, 0.65 mL (9.75 mmol) of thioglycolic acid was added dropwise to the stirring NaOH solution via a syringe through a rubber septum (the septum is used to contain the smell of the thioglycolic acid, not because the reaction is air sensitive). Next, 3.00 g (9.28 mmol) of 1-bromoacetylpyrene, dissolved in 90 mL of THF was added via syringe in a rapid dropwise fashion (approximately 5 to 10 drops a second). Once all chemicals were added, the round bottom flask was removed from the ice bath, covered in aluminum foil, and allowed to stir overnight at ambient temperature. Next, the solution was poured into a large beaker of ice, followed by the addition of 20 mL of concentrated hydrochloric acid and a yellow precipitate precipitated from solution. After the ice had melted, the precipitate was filtered off through fritted filter paper, then

washed with copious amounts of water (approximately 80 mL). After washing, the filter cake with water the filter paper was gently squeezed to wring out some of the excess water. Next, the yellow filtrate was redissolved in THF and subsequently evaporated to dryness under reduced pressure. The yellow solid was gently chopped into smaller pieces with a spatula and approximately 15 mL of chloroform was added. The flask was capped and placed in the freezer overnight. The following day the remaining yellow solid was filtered off and placed in a vacuum drying oven at 50 ^{o}C for 3 hours, yielding 2.09 g (67.4%) of the pyreneacyl sulfide acid precursor.

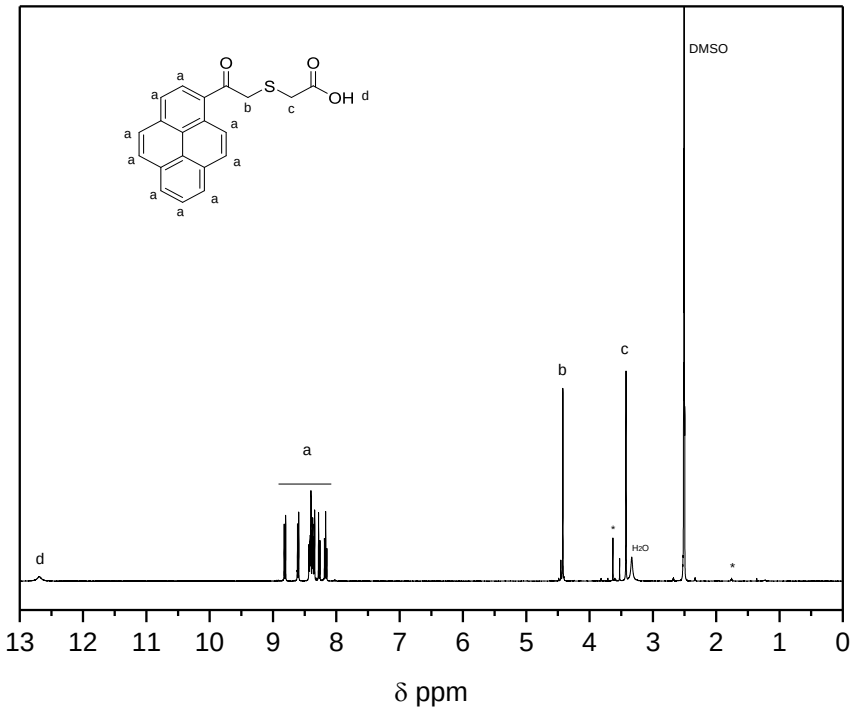

Figure S3: ^{1}H NMR of pyreneacyl sulfde acid. *Residual tetrahydrofuran. DMSO-d_6.

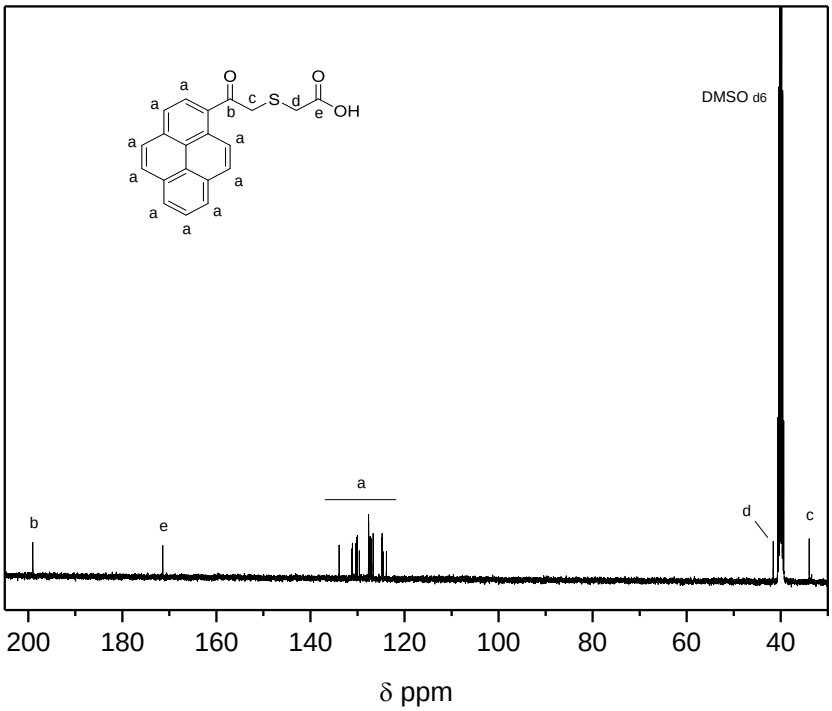

Figure S4: ^{13}C NMR of pyreneacyl acid precursor in DMSO-d_6.

Step 2: 0.1 g (0.3 mmol) of pyreneacyl sulfide acid from step 1 and 0.155 g (0.75 mmol) of N,N'-dicyclohexylcarbodiimide (DCC) were dissolved in 1 mL of extra dry DCM and added to a round bottom flask (RBF) capped with a rubber septum and subjected to magnetic stirring. Next, 0.3 g (0.15 mmol) of monomethoxy amine PEG (synthesized according to literature[2]) and 18.0 mg (0.15 mmol) of 4-dimethylaminopyridine (DMAP) were dissolved in 2 mL of extra dry DCM and then added dropwise, via a syringe to the stirring RBF containing the pyreneacyl sulfide/DCC solution. After all chemicals were added, the reaction was allowed to stir for 48 hours. Subsequently, the pyreneacyl sulfide terminated PEG was precipitated twice into cold (-10 °C) diethyl ether yielding 0.25 g (83.3%) of a light brown/yellow solid. SEC M_n = 2900 g mol^{-1}, $Đ$ = 1.06.

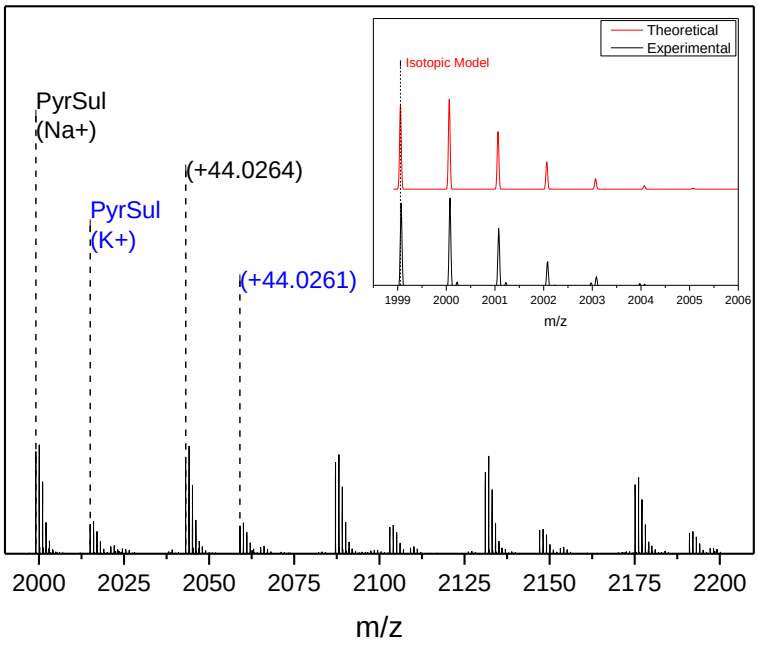

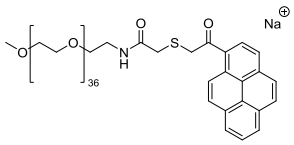

Resolution	m/z (exp)	m/z (theo)	Δ m/z
49702	1999.0718	1999.0572	0.0146

Figure S5: ESI-MS of pyreneacyl sulfide-PEG. Sodium and potassium adducts are observed.

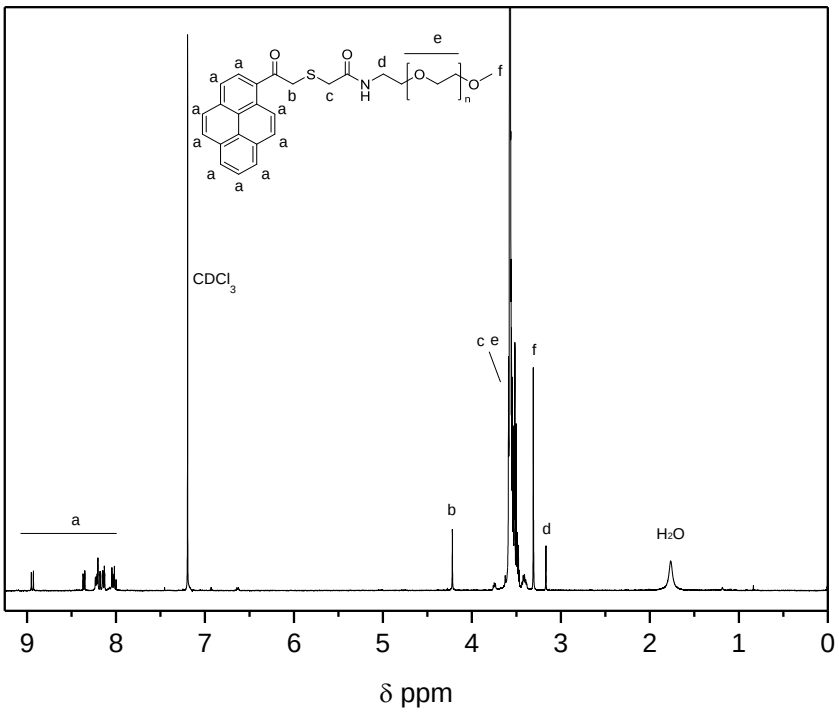

Figure S6 ^{1}H NMR of pyreneacyl sulfide-PEG in $CDCl_3$.

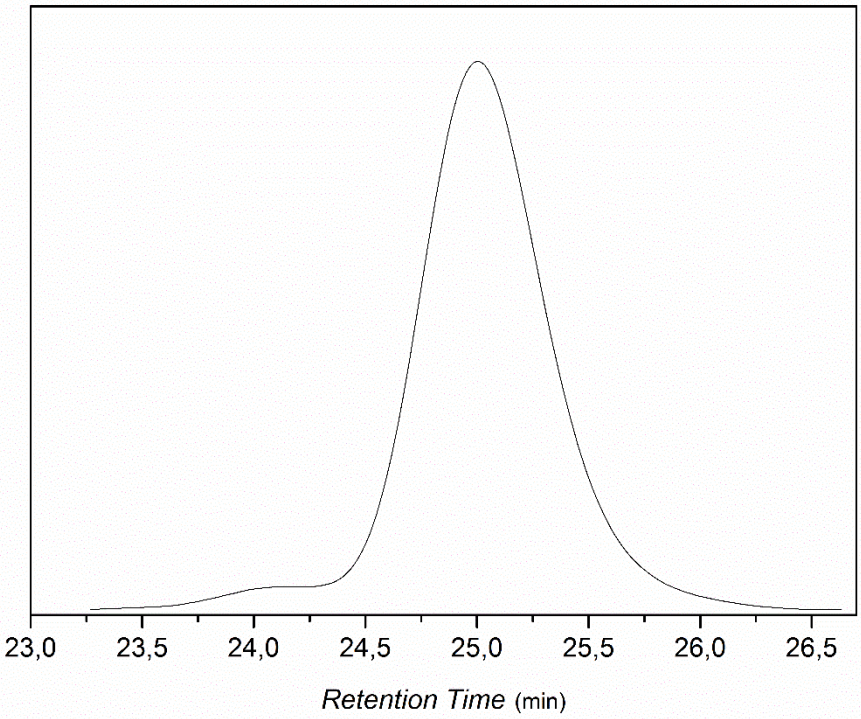

Figure S7: SEC of pyreneacyl sulfide-PEG in DMAc, 2 mg mL^{-1}, p(MMA) standards.

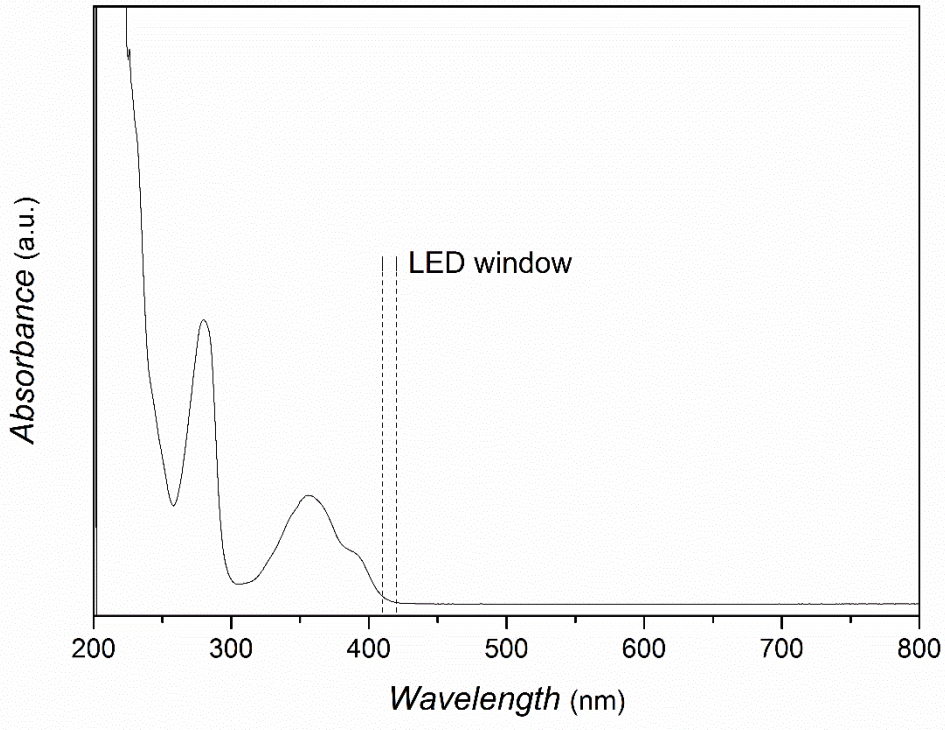

Figure S8: UV-Vis absorbance spectrum of pyreneacyl sulfide-PEG in 3:2 (v/v) THF/MeOH. LED emission window overlayed on spectrum.

Synthesis of visible light photo adducts

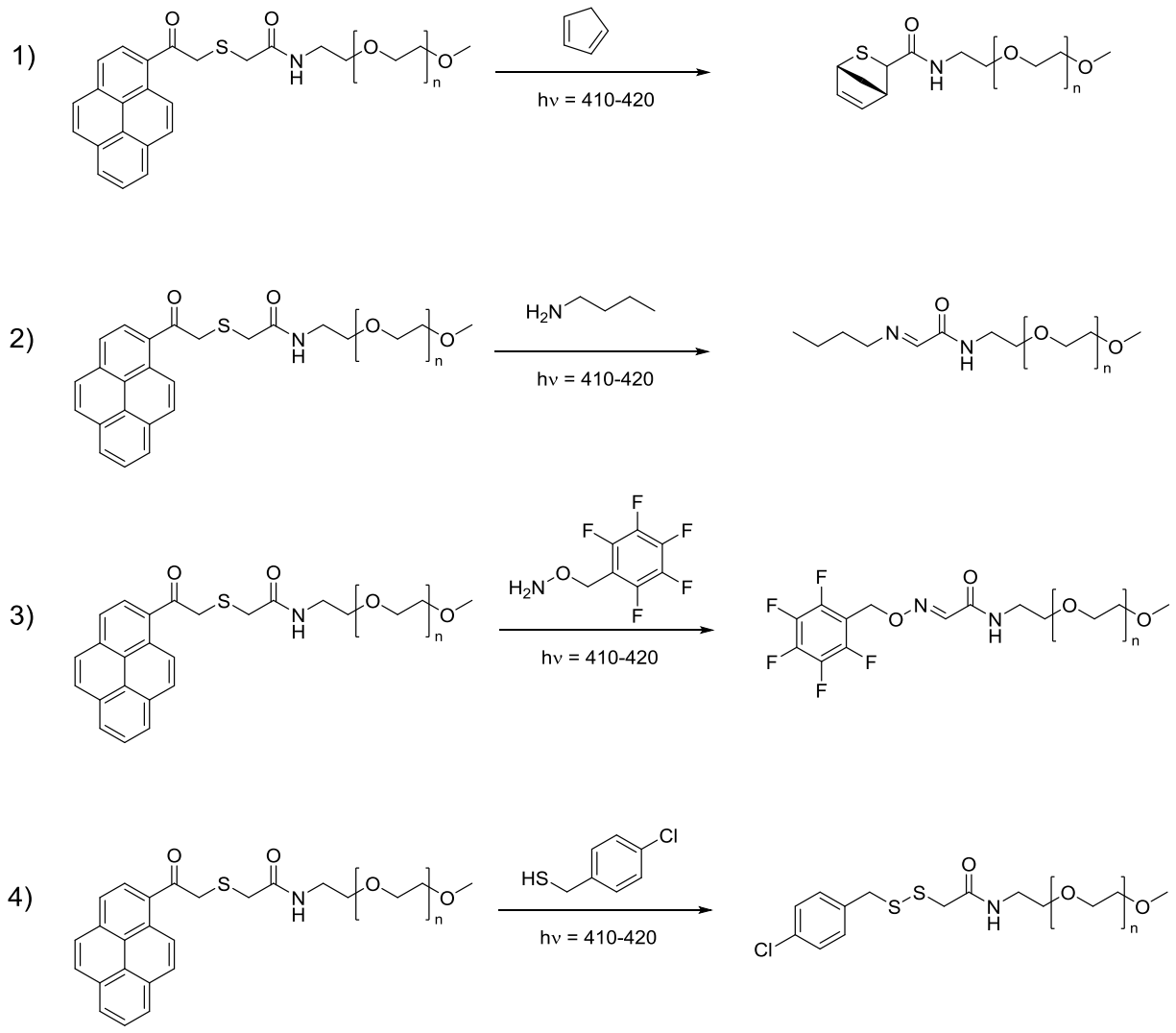

Scheme S2: Irradiation of pyreneacyl sulfide-PEG in the presence of various trapping agents.

Adduct 1: 1 mL of 0.05 mg mL^{-1} of pyreneacyl sulfide terminated PEG was dissolved in a THF/MeOH (3:2 v/v, containing 100 μmol sodium trifluoracetate) and placed in a glass scintillation vial. Next, 0.1 mL of freshly distilled cyclopentadiene was added to the scintillation vial along with a small magnetic stir bar. The solution was subsequently placed on a magnetic stirrer with three blue LEDs next to the vial according to Figure S1. The solution was then irradiated for 30 minutes. The solution, already at an appropriate concentration for ESI-MS analysis, was directly injected into the Orbitrap to confirm the successful photo-ligation.

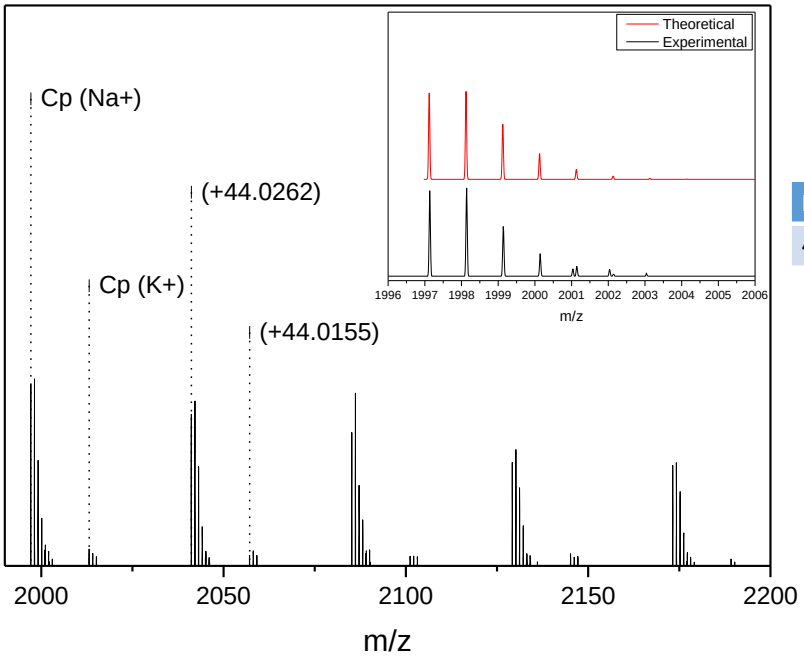

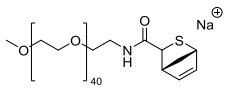

Resolution	m/z (exp)	m/z (theo)	Δ m/z
49602	1997.1360	1997.1202	0.0158

Figure S9: ESI-MS of adduct 1. Sodium and potassium adducts observed.

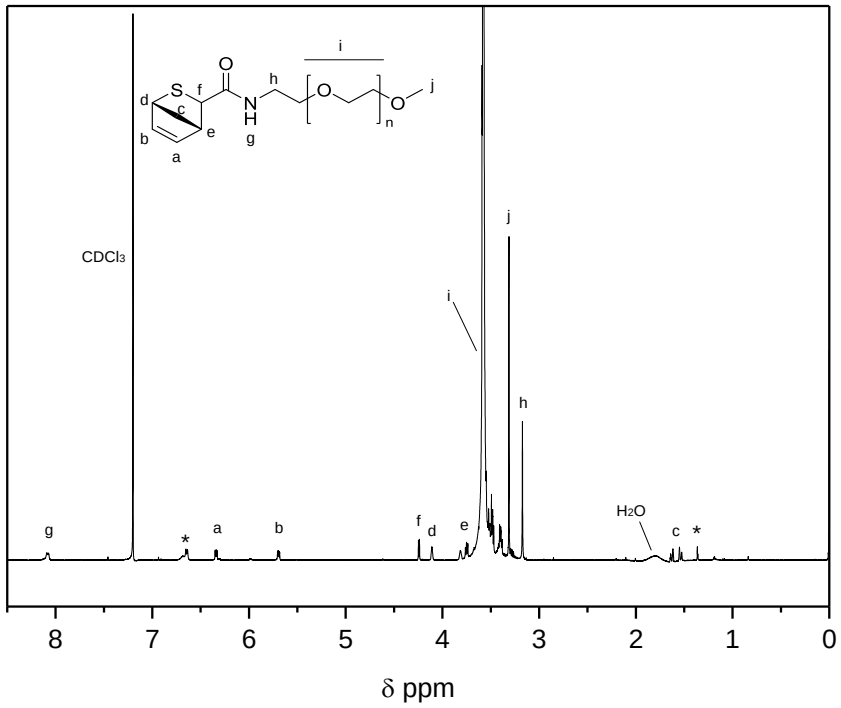

Figure S10: ^{1}H NMR of adduct 1. * Dicyclopentadiene impurities. $CDCl_3$.

Adduct 2: 1 mL of 0.05 mg mL^{-1} of pyreneacyl sulfide terminated PEG was dissolved in a THF/MeOH (3:2 v/v) and placed in a glass scintillation vial. Then a 0.1 mL aliquot of a 0.02 mM solution of butylamine in THF/MeOH (3:2, v/v, containing 100 μmol sodium trifluoracetate) was added to the scintillation vial along with a small magnetic stir bar. The solution was then placed on a magnetic stirrer with three blue LEDs next to the vial according to Figure S1. The solution was subsequently irradiated for 30 minutes. The solution, already at an appropriate concentration for ESI-MS analysis, was directly injected into the Orbitrap to confirm the successful photo-ligation. It should be noted here that no more than 1.2 equivalents of amine should be used as complete degradation of the photo-active moiety is observed, resulting in monohydroxy PEG.

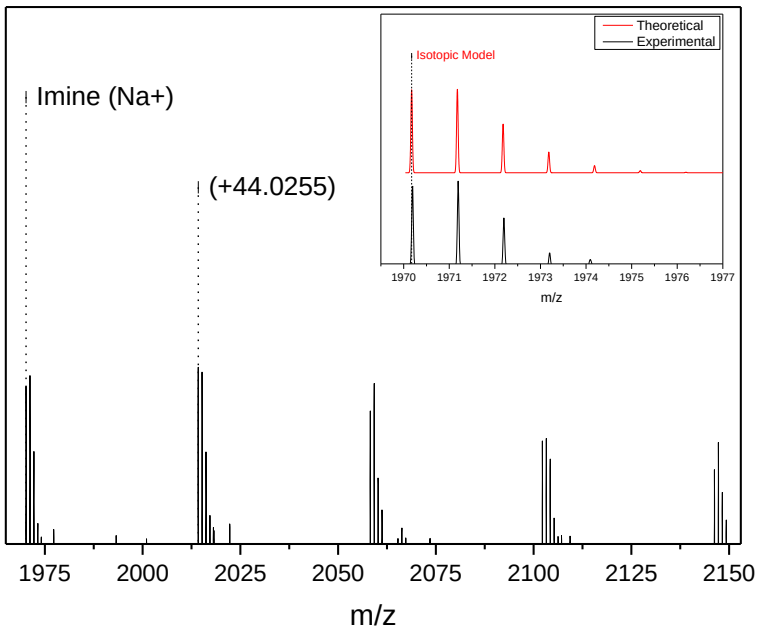

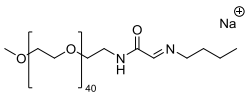

Resolution	m/z (exp)	m/z (theo)	Δ m/z
48202	1970.1942	1970.1746	0.0196

Figure S11: ESI-MS of adduct 2.

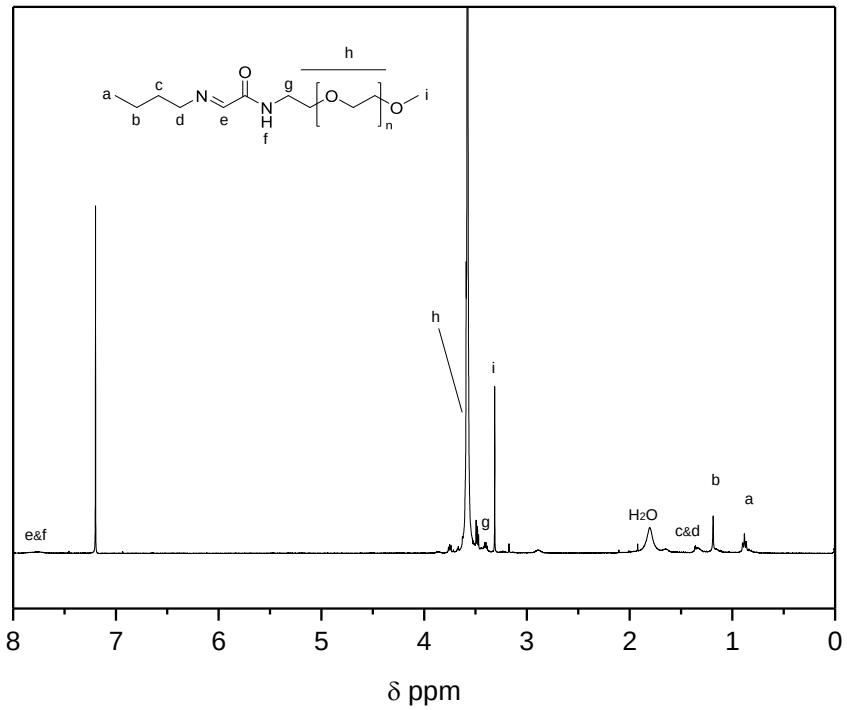

Figure S12: ^{1}H NMR of adduct 2. $CDCl_3$

Adduct 3: 1 mL of 0.05 mg mL^{-1} of pyreneacyl sulfide terminated PEG was dissolved in a THF/MeOH (3:2 v/v) and placed in a glass scintillation vial. Then a 0.1 mL aliquot of a 0.02 mM solution of O-2,3,4,5,6-pentafluorohydroxylamine hydrochloride in THF/MeOH (3:2, v/v, containing 100 μmol sodium trifluoracetate) was added to the scintillation vial along with a small magnetic stir bar. The solution was subsequently placed on a magnetic stirrer with three blue LEDs next to the vial according to Figure S1. The solution was then irradiated for 30 minutes. The solution, already at an appropriate concentration for ESI-MS analysis, was directly injected into the Orbitrap to confirm the successful photo ligation. It should be noted here that no more than 1.2 equivalents of hydroxylamine should be used as complete degradation of the photo-active moiety is observed, resulting in monohydroxy PEG.

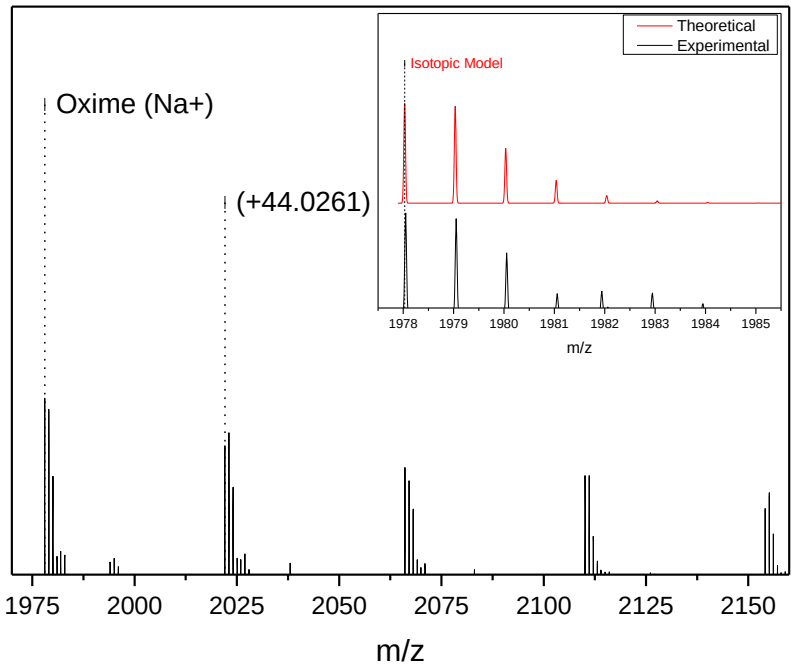

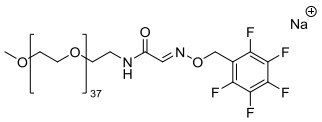

Resolution	m/z (exp)	m/z (theo)	Δ m/z
47706	1978.0482	1978.0282	0.0200

1

Figure S13: ESI-MS of adduct 3.

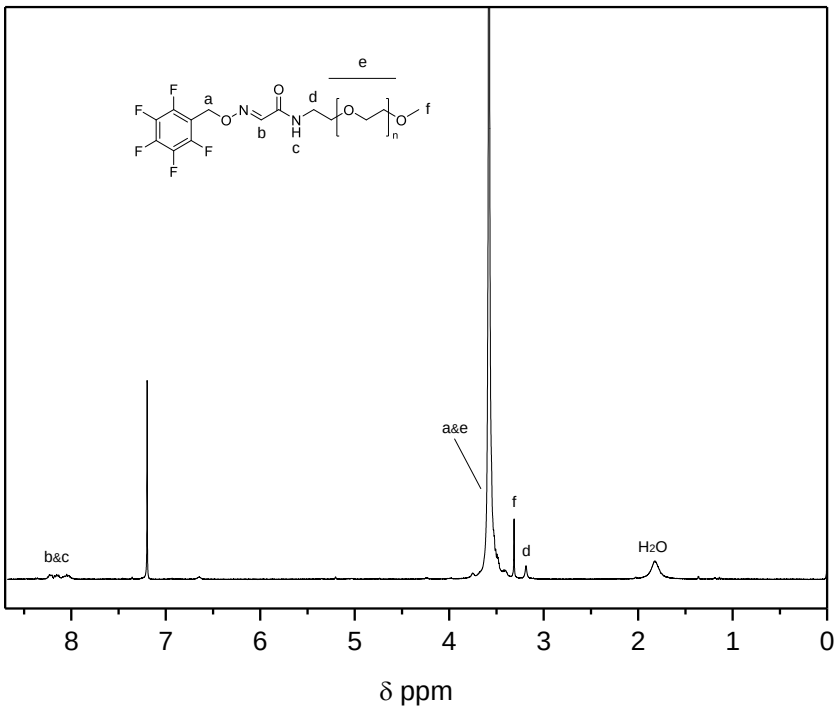

Figure S14: ^{1}H NMR of adduct 3 recorded in $CDCl_3$.

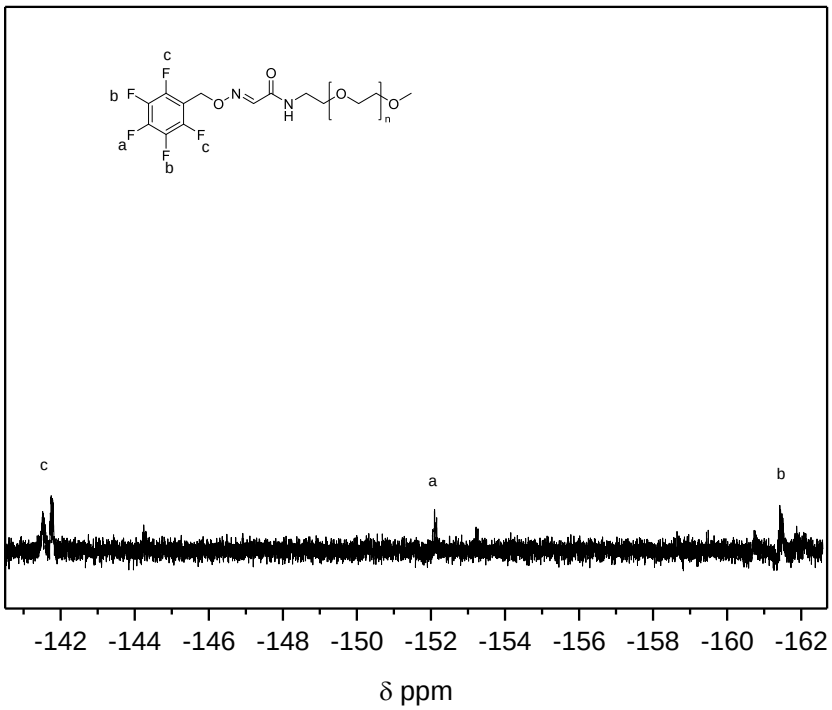

Figure S15: ^{19}F NMR of adduct 3 in $CDCl_3$.

Adduct 4: 1 mL of 0.05 mg mL^{-1} of pyrenacyl sulfide terminated PEG was dissolved in a THF/MeOH (3:2 v/v) and placed in a glass scintillation vial. Then a 0.1 mL aliquot of a 0.02 mM solution benzylchloro mercaptan in THF/MeOH (3:2, v/v, containing 100 μmol sodium trifluoracetate) was added to the scintillation vial along with a small magnetic stir bar. The solution was then placed on a magnetic stirrer with three blue LEDs next to the vial according to Figure S1. The solution was subsequently irradiated for 30 minutes. At the completion of irradiation 50 L of 35% hydrogen peroxide was added and stirred overnight to fully push the thiol/disulfide equilibrium to the disulfide form. The solution, already at an appropriate concentration for ESI-MS analysis, was directly injected into the Orbitrap to confirm the successful photo-ligation. Note: In the case of the disulfide formation, we are hesitant to commit to the statement that it is indeed a nucleophilic trapping. In our opinion, there is a complex proton transfer taking place between the thiol in solution and the thioaldehyde, resulting in the thioaldehyde being converted to a thiol, which is then subsequently oxidized to the disulfide.

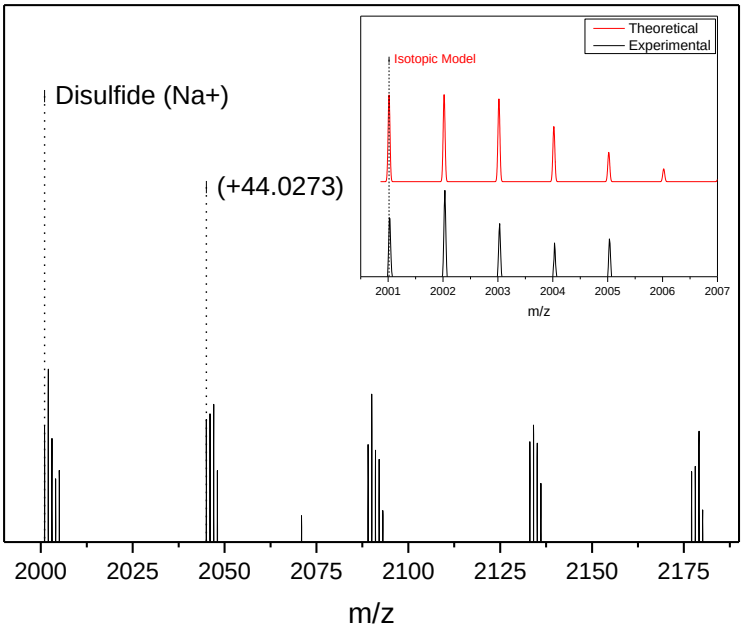

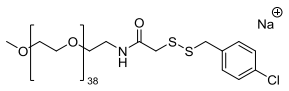

Resolution	m/z (exp)	m/z (theo)	Δ m/z
41702	2001.0270	2001.0165	0.0105

Figure S16: ESI-MS of adduct 4.

Visible light block copolymer synthesis

Synthesis of Cp²P^{t}BuA: The synthetic procedure was adapted from the literature.[3,4] 2,3 Bromo difunctional poly(*tert*-butyl acrylate) (1.0 eq., 3.4 g, 0.5 mmol), sodium iodide (6 eq. regarding bromo functionality, 971 mg, 6.5 mmol) and triphenyl phosphine (2 eq. regarding bromo functionality, 566 mg, 2.2 mmol) were dissolved in anhydrous THF (10.0 mL). Nickelocene (2 eq. regarding bromo functionality, 408 mg, 2.2 mmol) was added and the reaction mixture was stirred under argon at ambient temperature for 5 hours. The reaction was subsequently purged with air, filtered over basic aluminum oxide and the polymer was repeatedly precipitated in cold methanol/water 4:1. The off-white polymer was characterized via SEC, M_n = 4400 g mol^{-1}, $Đ$ = 1.10.

Synthesis of triblock (ABA) PEG-b-P^{t}BuA-b-PEG copolymer: 0.8 eq. of pyrenacyl sulfide PEG and 0.5 eq. of Cp_2PtuA (1 eq of cyclopentadiene) were added to a solution of 11 mL of THF and 0.05 mL of methanol (to aid the PEG solubility). The solution was allowed to stir for one hour (in the dark) to allow for sufficient mixing. After one hour of stirring, the solution was irradiated for 3.5 hours with blue LEDs. Upon completion of irradiation, the solvent was removed under reduced pressure to yield a pale yellow oil. This solution was then immediately reconstituted with 7 mL of DMAc and stirred for one hour, then analyzed via SEC, M_n = 5200 g mol^{-1}, $Đ$ = 1.16

3.) Tunable Laser Study

Tunable laser irradiation at constant photon count: As outlined in a previous publication from our team, the following protocol for achieving a constant photon count was employed.[5] Tunable UV laser light was generated by an Innolas Tunable Laser System SpitLight 600 OPO. An optical parametric

oscillator (OPO) was pumped with a diode pumped Nd:YAG laser (repetition rate 100Hz). The energy output of the laser was downregulated by a continuously variable attenuator (polarizer).

As shown in Scheme S3, the laser beam is redirected by a prism and enters the sample in a custom-made sample holder from below. The sample holder consists of a metal block with a vertical cylindrical hole (0.71 cm diameter), which can hold the vials used for the experiments. These are crimped 0.7 mL vials by LLG Labware, Lab Logistic Group GmbH (Art. Nr. 4-008202). The energy of the incident laser pulses was measured by an Energy Max PC power meter (Coherent).

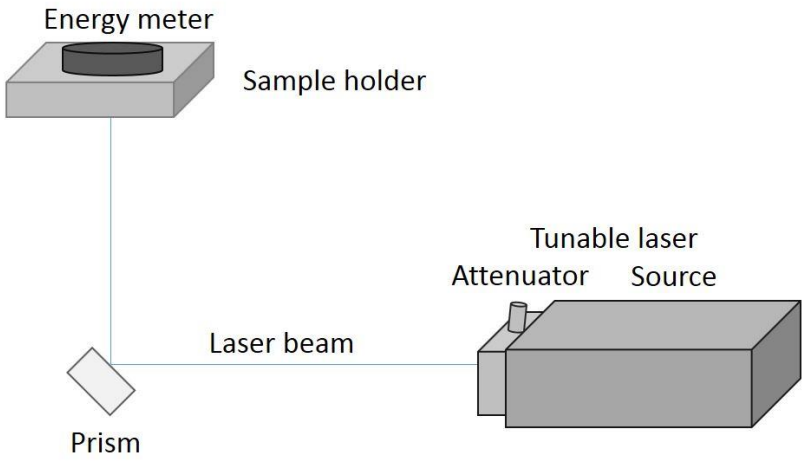

Scheme S3: Experimental setup for the measurement of the laser energy.

Transmittance of glass vials: The transmittance of the glass vials that were used for photoreactions with the tunable laser system was determined experimentally using the tunable laser setup. Measurement of the energy of laser pulses at a constant energy output was carried out directly above the sample holder first without a glass vial in the sample holder and subsequently with an empty glass vial in the sample holder. The top part of the glass vials, shown in Figure S17, was removed for these measurements. Thus, only the absorbance of the bottom of the vial is detected. The obtained values are shown in Table S1. The described procedure was performed for three individual glass vials to account for variabilities between the vials.

Figure S17: Uncrimped vial; left: vial after removal of head space section.

Table S1: Transmittance of glass vials

λ / nm	mean transmittance / %	mean deviation / %
270	0	0
275	0	0
280	0	0
285	13.4	0.2
290	19.7	0.6
295	30.3	0.5
300	37.7	1.0
305	45.6	0.5
310	47.5	1.0
315	51.1	0.6
320	56.3	1.2
325	58.9	0.8
330	61.0	0.9
335	62.9	0.9
340	60.4	0.9
345	64.5	1.6
350	60.4	1.1
355	62.1	0.9
360	65.1	0.3
370	65.9	1.2
380	66.3	1.2
390	70.8	0.4
400	66.9	0.9
410	68.0	1.9
430	75.3	0.6
450	76.6	0.8
470	77.6	0.5
490	79.1	0.5

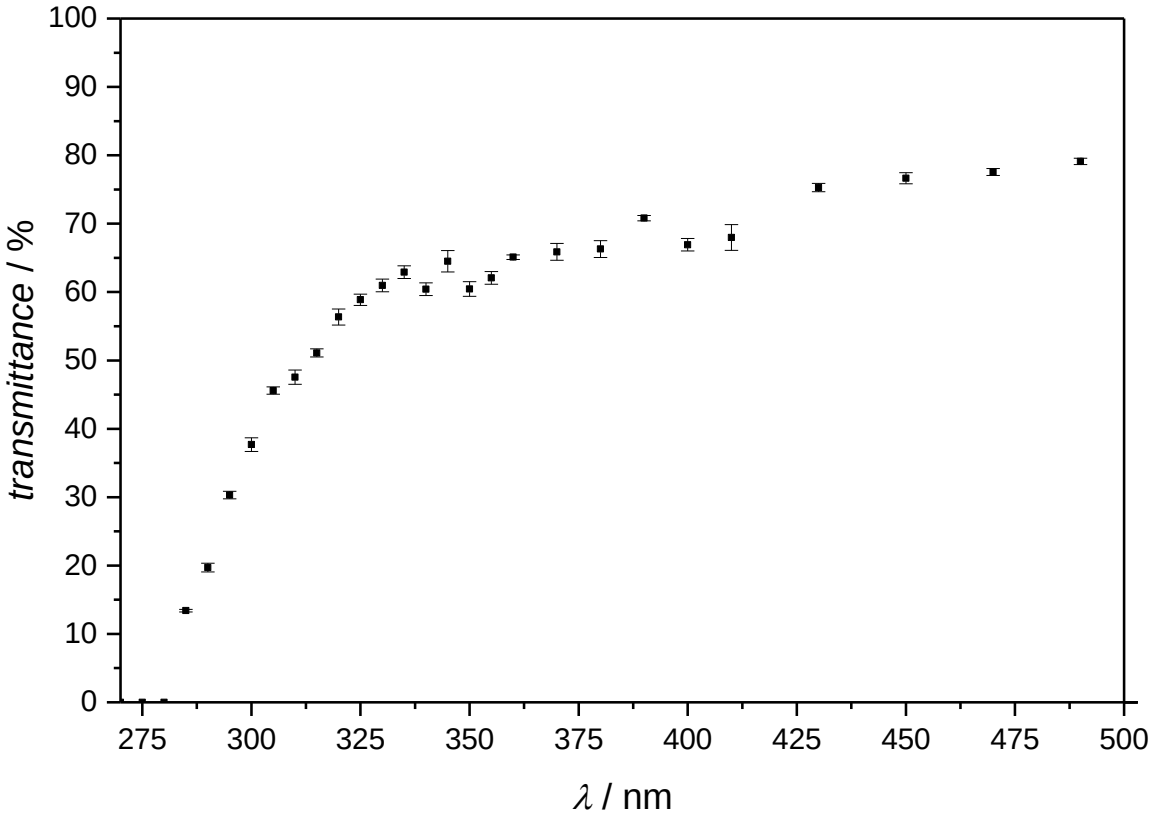

Figure S18: Transmittance of glass vials dependent on irradiation of wavelength.

Irradiation at constant photon count: For all irradiation wavelengths, a 'target energy' was calculated. The target energy per pulse E^0 was defined as the measured energy in case of an empty sample holder. For each irradiation experiment the attenuator position, defined and controlled by the measurement of E^0, enables irradiation of each sample solution with a defined number of photons. The target energy per pulse E^0 is calculated directly from the wavelength λ, the number of pulses k, the transmittance of the glass vial at the respective wavelength T_λ and the desired total photon count $n_{h\nu}$.

$$E^0 = \frac{n_{h\nu} * h * c}{k * T_\lambda * \lambda}$$

Thus, the number of photons penetrating the respective sample solutions is identical.

Wavelength dependence of the pyreneacyl sulfide photolysis: 8.99 mg (3.96 µmol, 1.00 eq.) α-methyl-ω-(2-((2-oxo-2-(pyren-1-yl)ethyl)thio)acetamido) poly(ethylene glycol) were dissolved in 4.5 mL tetrahydrofuran/methanol 3:2 (v/v), containing 0.1 mmol L^{-1} sodium trifluoroacetate. 0.71 mg (10.7 mmol, 2750 eq.) Cyclopentadiene was added to the solution. Each 0.1 mL aliquots were irradiated with 5.0 µmol photons of variable wavelength per the above described procedure. Irradiation was carried out in the range from 285 nm to 435 nm in 15 nm steps. Samples were generally shielded from daylight and all light sources other than the intended tunable laser irradiation. Conversion was determined *via* high resolution electrospray ionization mass spectrometry. Each solution was filtrated, diluted with 0.1 mL tetrahydrofurane/methanol 3:2 (v/v), containing 0.1 mmol L^{-1} sodium trifluoroacetate and infused into the mass spectrometer at a flow of 5 µL min^{-1}. Spray voltage was set to 4.6kV and the sweep gas flow rate to 5 (dimensionless parameter). A capillary temperature of 320°C and an S-lens RF level of

62.0 were applied. An average of the signal over 40 scans was obtained. The conversion was calculated from the double charged region of the spectrum in a mass to charge ratio range from 1100 Da to 1500 Da (47 to 57 repeating units) per the procedure described in the section “Semi-automated quantitative analysis of polymer mass spectra”.

Table S2: Observed apparent conversion

λ / nm	p / %
285	43.6
300	19.0
315	46.9
330	55.2
345	61.7
360	79.6
375	74.3
390	57.8
405	49.7
420	24.4
435	1.5

Semi-automated quantitative analysis of polymer mass spectra: The determination of the apparent conversion regarding the photolysis of poly(ethylene glycol) bound pyreneacyl sulfide and subsequent Diels Alder cycloaddition with cyclopentadiene from high resolution electrospray ionization mass spectra is described below. A sample, which was irradiated with light of the wavelength 375 nm, is discussed as an example.

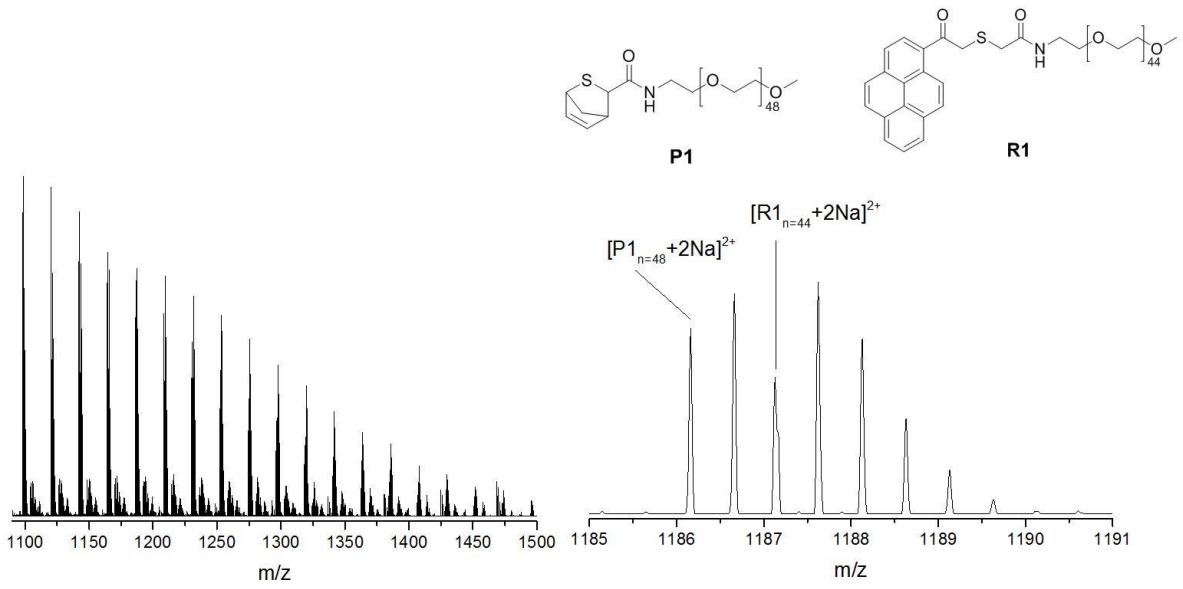

Figure S19 Mass spectrum of the reaction mixture of PEG-pyrene acyl sulfide and cyclopentadiene after irradiation with 375 nm. Left: Double charged region of the mass spectrum; Right: The reactant R1 and product P1.

Table S3 Example reactant and product signal in mass spectrum

species	experimental m/z	simulation	R
$[R1_{n=44}+2Na]^{2+}$	1187.127	1187.1281	28100
$[P1_{n=48}+2Na]^{2+}$	1186.1594	1186.1595	32102

An algorithm for the analysis was written in the programming language Python. The program reads a respective mass spectrum as an Excel file (list of mass to charge ratios and relative intensities), determines the apparent conversion in dependence of the number of repeating units and calculates the average apparent conversion from suitable values. The algorithm can be divided into various modules, which are carried out successively. An overview is shown in Scheme S4.

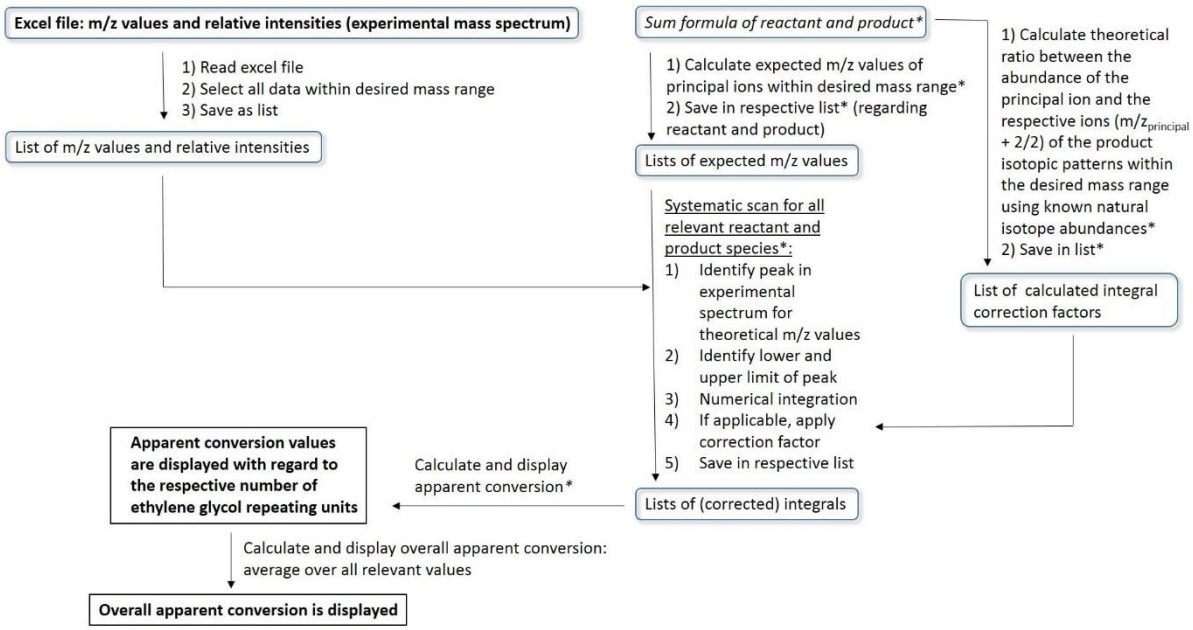

Scheme S4: Graphical representation of the performed numerical mass spectral analysis.

The peak of the principal ion of each relevant isotope pattern is identified and integrated numerically. The lower and upper limit for integration are defined by the intensity taking the value zero. Due to an overlap of the two species the integral of the peak of the reactant needs to be corrected (see Figure S19). Calculation of the expected relative intensities of the first (principal ion) and third peak of the product isotopic pattern was carried out for each relevant species to obtain the true values. Exact mass and natural abundance of isotopes were used for the calculation (see Table S4). Combinations of isotopes that contribute to the first and third peak of the isotopic pattern are shown in Table S5. These were used to calculate the theoretical ratio of the integrals of the peaks.

Table S4: Relevant isotopes, exact mass and natural abundance values

Isotope	exact mass m / amu	abundance a / %
^{1}H	1.0078	99.9885
^{2}H	2.0141	0.0115
^{12}C	12.0000	98.93
^{13}C	13.0034	1.07
^{14}N	14.0031	99.636
^{15}N	15.0001	0.364
^{16}O	15.9949	99.7
^{17}O	16.9991	0.04
^{18}O	17.9992	0.2
^{32}S	31.9721	94.93
^{33}S	32.9715	0.76
^{34}S	33.9679	4.29

Table S5: General isotopic composition of relevant species contributing to the first (species 15) and third (species 1 to 14) peak of isotopic patterns of PEG-thiabicycloheptane with the general formula $C_mH_nN_oO_pS_g$

Species	^{12}C	^{13}C	^{1}H	^{2}H	^{14}N	^{15}N	^{16}O	^{17}O	^{18}O	^{32}S	^{33}S	^{34}S
1	m	0	n	0	o	0	p	0	0	q-1	0	1
2	m	0	n	0	o	0	p-1	0	1	q	0	0
3	m-1	1	n	0	o-1	1	p	0	0	q	0	0
4	m-1	1	n	0	o	0	p	0	0	q-1	1	0
5	m	0	n	0	o-1	1	p	0	0	q-1	1	0
6	m	0	n	0	o-1	1	p-1	1	0	q	0	0
7	m	0	n	0	o	0	p-1	1	0	q-1	1	0
8	m-2	2	n	0	o	0	p	0	0	q	0	0
9	m	0	n-1	1	o-1	1	p	0	0	q	0	0
10	m	0	n-1	1	o	0	p	0	0	q-1	1	0
11	m-1	1	n	0	o	0	p-1	1	0	q	0	0
12	m-1	1	n-1	1	o	0	p	0	0	q	0	0
13	m	0	n-1	1	o	0	p-1	1	0	q	0	0
14	m	0	n-2	2	o	0	p	0	0	q	0	0
15	m	0	n	0	o	0	p	0	0	q	0	0

The apparent conversion is calculated for each chain length from the respective corrected integrals. Figure S20 shows the plot of the apparent conversion against the number of repeating units. The ionization bias of the end group is responsible for the deviations that occur for low numbers of repeating units. An average apparent conversion is finally calculated from the apparent conversion values, which are in the linear region of the plot shown in Figure S20. Thus, the influence of the ionization bias of the end group is minimized.

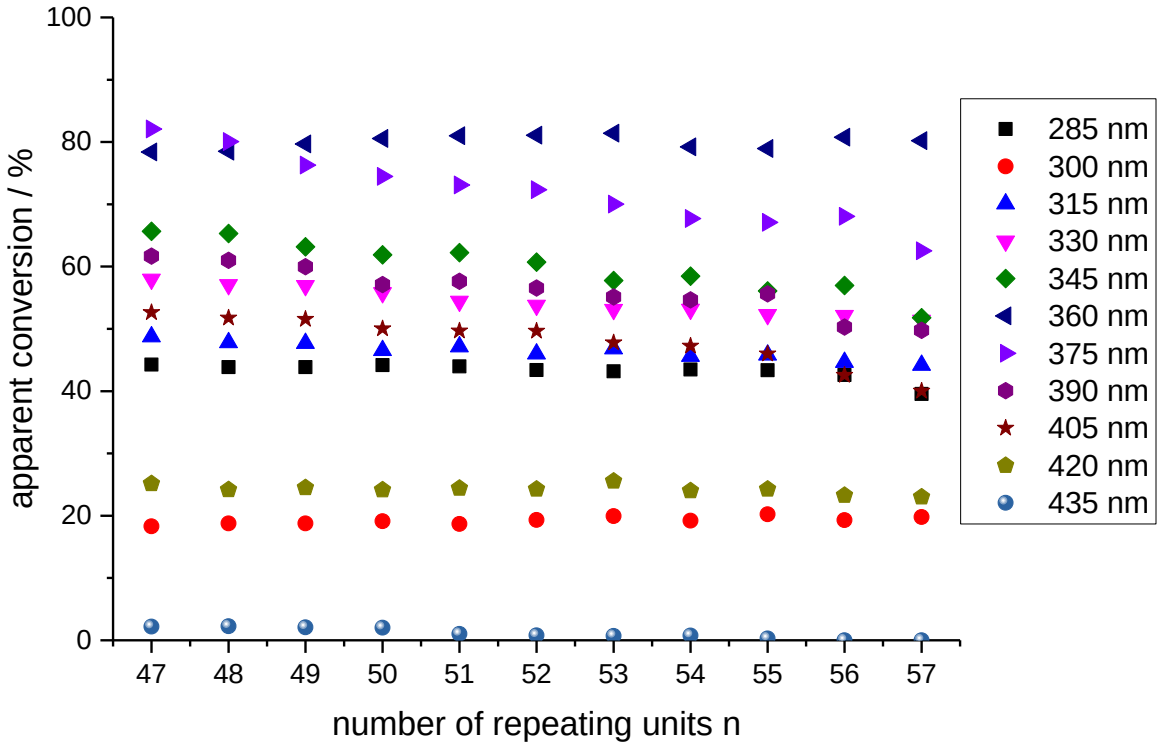

Figure S20: Apparent conversion plotted against the number of repeating units, n.

Wavelength independent formation of thiabicycloheptene: 2.4 mg (1.0 µmol, 1.00 eq.) α-methyl-ω-(2-((2-oxo-2-(pyren-1-yl)ethyl)thio)acetamido) poly(ethylene glycol) were dissolved in 1.2 mL tetrahydrofurane/methanol 3:2 (v/v), containing 0.1 mmol L^{-1} Sodium trifluoroacetate. 0.236 g (3.57 mmol, 3430 eq.) cyclopentadiene were added to the solution. Each 0.1 mL were irradiated with varying numbers of photons (refer to Table S3) per the procedure described previously. Samples were generally shielded from daylight and all light sources other than the intended tunable laser irradiation.

Table S6: Irradiation parameters

Sample	Irradiation wavelength λ / nm	Number of pulses n_{pulses} / a.u.	Number of incident photons $n_{photons}$ / µmol
1	285	200000	25.2
2	300	100000	50.5
3	315	100000	25.2
4	330	90000	22.7
5	345	80000	20.2
6	360	50000	12.6
7	375	50000	12.6
8	390	90000	22.8
9	405	50000	25.1
10	420	20000	50.4
11	435	200000	504

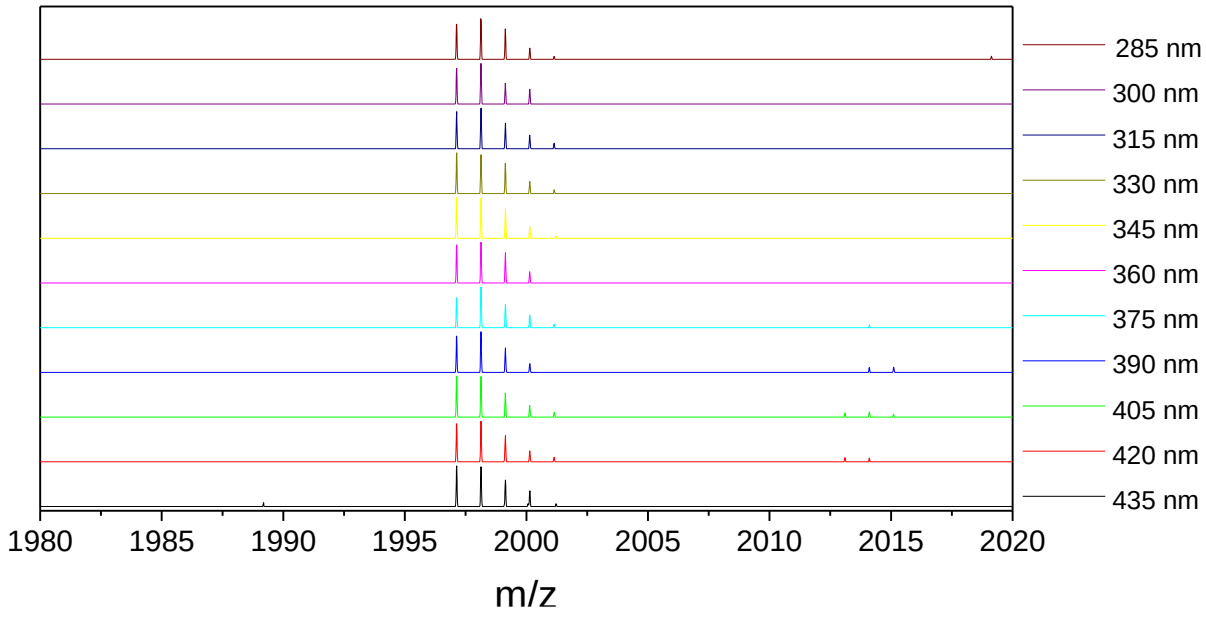

Figure S21: Wavelength independent formation of adduct 1

High resolution electrospray ionization mass spectrometry: The solution was filtrated, diluted with 0.1 mL tetrahydrofuran/methanol 3:2 (v/v), containing 0.1 mmol L^{-1} Sodium trifluoroacetate and infused into the mass spectrometer at a flow of 5 µL min^{-1}. Spray voltage was set to 4.6kV and the sweep gas flow rate to 5 (dimensionless parameter). A capillary temperature of 320°C and an S-lens RF level of 62.0 were applied. An average of the signal over 40 scans was obtained.

References

1 A. Rudin and H. L. W. Hoegy, *J. Polym. Sci. Part A-1 Polym. Chem.*, 1972, **10**, 217–235.

2 P. Mongondry, C. Bonnans-Plaisance, M. Jean and J. F. Tassin, *Macromol. Rapid Commun.*, 2003, **24**, 681–685.

3 K. Pahnke, J. Brandt, G. Gryn'ova, C. Y. Lin, O. Altintas, F. G. Schmidt, A. Lederer, M. L. Coote and C. Barner-Kowollik, *Angew. Chemie Int. Ed.*, 2016, **55**, 1514–1518.

4 K. Pahnke, J. Brandt, G. Gryn'ova, P. Lindner, R. Schweins, F. G. Schmidt, A. Lederer, M. L. Coote and C. Barner-Kowollik, *Chem. Sci.*, 2015, **6**, 1061–1074.

5 C. Fast, D. E.; Lauer, A.; Menzel, J. P.; Kelterer, A.-M.; Gescheidt, G.; Barner-Kowollik, *Macromolecules*, 2017, DOI: 10.1021/acs.macromol.7b00089.